Supplementary Appendix

This appendix has been provided by the authors to give readers additional information about their work.

Supplement to: Albert JS, Yerges-Armstrong LM, Horenstein RB, et al. Null mutation in hormone-sensitive lipase gene and risk of type 2 diabetes. N Engl J Med 2014;370:2307-15. DOI: 10.1056/NEJMoa1315496

TABLE OF CONTENTS

SUPPLEMENTAL METHODS

Study population:

The Old Order Amish (OOA) of Lancaster County, PA is a founder population that our group has been studying since 1993. The current Lancaster OOA population numbers ~34,000 individuals, including ~12,000 adults. We have estimated that these individuals are descendants of just 554 founders, with 128 of these founders contributing to 95% of the present day gene pool.[1] Through the leadership of coauthor Dr. Alan Shuldiner, we had as of 4/19/13 enrolled into one or more of our studies 4,535 Amish adults with DNA samples, ~4,000 of whom have extensive phenotype information in one or more of the following areas: glucose homeostasis/diabetes, cardiovascular health, bone health, longevity, and platelet function and response to anti-platelet agents. This rich collection of well-phenotyped subjects makes up the Amish Complex Disease Research Program (ACDRP). For our study, we selected 2738 of these subjects for whom we had both HSL genotype and relevant phenotype information [Specifically, the main data set included only subjects with non-missing values for body mass index (BMI), and serum LDL-cholesterol, HDL-cholesterol and triglycerides (TG).], most of whom participated in one or more of the following studies:

Amish Family Diabetes Study (AFDS): The AFDS was initiated in 1995 to identify susceptibility genes for type 2 diabetes (T2D).[2] Phenotypic characterization included a detailed medical exam including blood pressure, anthropometry, a standard fasting lipid panel, and a 3-hour 75-gram oral glucose tolerance test (OGTT) with insulin levels.

Amish Family Calcification Study (AFCS): The AFCS was initiated in 2001 to identify the determinants of vascular calcification and to evaluate the relationship between calcification of bone and vascular tissue.[3] Subjects underwent a detailed medical examination including blood pressure, anthropometry, a standard fasting lipid panel, and the measurement of coronary artery calcification (CAC) by electron bean computed tomography (EBCT).

Amish Family Longevity Study (AFLS): The AFLS was established in 2001 to identify genes that influence longevity and longevity-related traits in humans.[4] Long-lived Amish probands (age > 90) were identified using the Amish Genealogical Database and through surveys sent to all Amish households listed in the Amish Church Directory (Church Directory of Lancaster County Amish, 1996) and recruited to the study along with all willing offspring and spouses of offspring. Phenotypic characterization included a detailed medical exam including blood pressure, anthropometry, and a standard fasting lipid panel.

Heredity and Phenotype Intervention (HAPI) Heart Study: The HAPI Heart Study began in 2003 to identify genes that interact with environmental exposures to influence risk for cardiovascular disease.[5] Subjects underwent a detailed medical examination including blood pressure, anthropometry, a standard fasting lipid panel and four short-term interventions designed to challenge cardiovascular function including blood pressure responses to (1) the cold pressor stress test and (2) a high salt diet, (3) triglyceride excursion in response to a high fat challenge, and (4) response in platelet aggregation to aspirin therapy.

Pharmacogenomics of Antiplatelet Intervention (PAPI) Study: The Amish PAPI Study was initiated in 2006 to identify genetic variants that influence the efficacy of oral antiplatelet agents (e.g. aspirin and clopidogrel).[6] In addition to a detailed medical exam including blood pressure, anthropometry, and a standard fasting lipid panel, subjects underwent an 8-day clopidogrel treatment with platelet aggregation studies pre- and post-treatment and 1 hour after ingestion of 324 mg aspirin on day 8.

Pharmacogenomics of Thiazolidinedione Response: This study was active from 2007-2013 and was designed to identify the determinants of responsiveness to pioglitazone, an oral hypoglycemic agent. Subjects were overweight or obese, but otherwise healthy. Adipose tissue biopsies and intravenous glucose tolerance tests were performed at baseline and after 12 weeks of pioglitazone therapy.

The above study protocols were approved by the Institutional Review Board at the University of Maryland, and all subjects gave written informed consent.

Phenotype measurements:

Standardized protocols and procedures were used for all phenotyping across all studies. Height and weight were measured using a stadiometer and calibrated scale, and BMI (kg/m^2) was computed. Fasting serum TG, total cholesterol and HDL-cholesterol were measured by Quest Diagnostics (Horsham, PA). LDL-cholesterol was calculated by the Friedewald equation where TG < 400 mg/dl.[7] Glucose concentrations were assayed with a glucose analyzer (Beckman Coulter, Brea, CA or YSI, Yellow Springs, OH). Insulin levels were determined by radioimmunoassay (Linco Research Inc., St. Charles, MO). HOMA-IR was calculated using the following formula: HOMA-IR = [Fasting glucose (in mg/dl)*Fasting insulin (in µU/ml)]/405. Total glucose (gAUC) and insulin (iAUC) area under the curve were calculated using the trapezoidal method based on measurements at 0, 30, 60, 90, 120, 150, and 180 minutes during the OGTT.[2] Diabetes was defined by fasting plasma glucose level ≥ 126 mg/dl, random or 2-hour OGTT glucose ≥ 200 mg/dl, the use of insulin or prescription oral glucose-lowering agents, or a previous diagnosis of diabetes documented by a physician. Normal glucose tolerance was defined by fasting glucose <100 mg/dl and 2-hour OGTT glucose < 140 mg/dl.[8] Hypertriglyceridemia was defined by TG > 150 mg/dl as outlined by AHA/NCEP criteria.[9] Systolic and diastolic blood pressures were obtained in triplicate using a standard sphygmomanometer with the subject sitting for at least 5 minutes. Hypertension was defined as ≥ 130 / ≥ 85 mmHg using the ATP III criteria for metabolic syndrome.[10]

Electron-beam computerized tomography (EBCT):

Hepatic fat content (reported as spleen:liver density ratio with a higher ratio indicating more fat) was measured in a subset of subjects by thoracic EBCT scans on an Imatron C-150 EBCT scanner.[11] Two 1.0 cm^2 regions of interest (ROI) were measured for the liver and one was measured from the spleen in a manner that minimized measurements of vessels, focal lesions, artifacts or the edge of the organ. Accu View (Accuimage Corp.) software was used to calculate the attenuation coefficient in Hounsfield Units for each ROI. The spleen measure was divided by the average of the two liver attenuation measurements to calculate spleen:liver ratio. All scans were performed and analyzed blinded to *LIPE* genotype.

Due to strict cultural and religious principles, alcohol consumption in the Amish population is frowned upon and very rare and thus we believe unlikely to confound our measurements of liver fat. In order to maintain cultural sensitivity to this point, we do not ask about alcohol consumption.

Dual-energy x-ray absorptiometry (DXA):

Whole body and regional percent fat were analyzed and compared by DXA in a subset of 42 II and 7 ID females matched on total body percent fat and age to the 3 DD females. Total mass, fat mass and total percent fat measures were acquired from whole body DXA scans using a Hologic 4500W (Hologic, Bedford, MA) and daily phantom measurements were obtained to detect measurement shifts over time. The android region was defined as 20% of the region between the neck cut line and the pelvic cut line and rested atop the pelvic cut line. The gynoid region was 2x the height of the android region and placed below the android region by 1.5x the android region height. The arm and leg regions were calculated by averaging together the right and left arms or legs, respectively. The “upper leg” was measured from the top of the femoral head to the knee joint and the “lower leg” was measured from the knee joint to the ankle joint. All scans were performed and analyzed blinded to *LIPE* genotype.

Magnetic resonance imaging (MRI):

The DD proband and her siblings were invited to participate in MRI studies for further characterization of fat deposition and body composition. Two siblings declined, so a total of 8 MRI studies were performed. All MR images were acquired on a 1.5T Siemens Avanto scanner, with version B-17 of the scanner software. All patients were imaged in the supine position. All scans were performed and analyzed blinded to *LIPE* genotype. Acquired images and spectra were independently analyzed by two researchers (ASR and RJB), and the results averaged.

<u>*Hepatic fat quantification:*</u> Heavily T1 weighted breath hold images were acquired with a 6 channel phased array body coil. The entire liver was interrogated using a multiecho gradient echo sequence with the following

parameters: flip angle 10 degrees, echo time (TE) = 2.3, 4.6, 6.9, and 9.2 milliseconds, relaxation time (TR) =150 ms, and slice thickness= 8 mm with 100% gap. The acquired images were imported into AqNET thin client (Tera Recon, Foster City, CA), which automatically coregistered the images acquired at a given axial position, and propagated the regions of interest (ROI) used for quantification of signal intensity. Three random ROIs were manually selected in different axial locations, taking care to avoid large vascular and biliary structures, edges of the liver and any focal fatty infiltration. The signal intensity of the first out of phase ROI, and the first and second in phase ROIs were determined. Quantification of hepatic fat was then separately calculated for each ROI using the triple echo technique described by Yokoo et al[12], and the results were averaged.

Visceral/subcutaneous adipose tissue quantification: A total of two breath hold T1 weighted gradient echo images (with and without fat suppression) were acquired at the L4 - 5 disk space using a 6 channel phased array body coil. The field of view included all skin surfaces. Scan parameters were: flip angle 70 degrees, TE = 4.6 ms, TR = 150 ms, slice thickness 10 mm, and in plane voxel size 2 x 2 mm. ImageJ (NIH, Bethesda, MD) was utilized for analysis. The fat suppressed image was subtracted from the non-fat suppressed, thereby nulling any inherently T1 bright non-adipose tissues. The minimum signal intensity of fat was then determined. Segmentation of visceral and subcutaneous regions was carried out using freehand ROIs. The number of pixels with signal intensity greater than the previously determined minimum signal intensity for fat, in conjunction with the in plane spatial resolution of the images, was used to compute the number of square millimeters of fat in each compartment.

The subcutaneous fat in the calf of each subject was quantified using ImageJ (NIH, Bethesda, MD). A ROI was drawn using the freehand selection tool, and the included area was measured using the Measure option under the Analyze menu. The results of three trials for each of two researchers (AR and RB) was averaged and reported.

***Sequencing and genotyping*:**

PCR was performed to amplify all exons in twelve genes in the lipolytic pathway (*PNPLA2, ABHD5, LIPE, MGL, PLIN1, PLIN2, PLIN3, PLIN4, PLIN5, SERPINF1, LPL,* and *GPIHBP1)* in 24 Amish subjects, 12 with extremely high and 12 with extremely low fasting serum TG (lower extreme: median = 23.6 mg/dl, range = 14 - 25 mg/dl; upper extreme: median = 298.0 mg/dl, range = 273 - 608 mg/dl). Cycle sequencing of the purified PCR products was performed on the ABI Prism 3730 Genetic Analyzer following a standardized protocol (Applied Biosystems, Foster City, CA). The Sequencher version 4.5 software (Gene Codes Corporation, Ann Arbor, MI) was used to analyze the sequence and identify sequence variation.

Genotyping was performed using PCR amplification of the region containing the newly identified 19 base pair deletion (p.V767Gfs*102) using the forward primer 5'-CACGGCTTCCTGACCCTA-3' and reverse primer 5'-CCGACTTAAGTAAGGCACAGC-3', electrophoresis on a 3% agarose gel and visualization under ultraviolet light. The wild-type product was 253 bp in length. Genotyping in 2738 Amish samples from our ACDRP identified 140 ID subjects and 1 DD proband (Amish D allele frequency = 2.6%). We also identified 3 IDs among 1730 non-Amish Caucasian subjects (allele frequency = 0.1%), thus establishing the existence of the allele outside the Amish and demonstrating the enrichment of this allele in the Amish through a founder effect. All genotyping included at least 5% duplicate samples to determine mistyping rates which were <1%.

Adipose tissue collection and processing:

Abdominal subcutaneous adipose tissue biopsies were obtained by aspiration from 7 subjects homozygous for the wild type allele (II), 10 subjects heterozygous for the deletion (ID) and 2 subjects homozygous for the deletion (DD) using a 2.5 mm cannula under local lidocaine anesthesia as previously described.[13] Tissue was immediately snap frozen in liquid nitrogen for extraction of RNA and protein or was placed in PBS for transport to the laboratory for preparation of isolated adipocytes.

Lipolysis: Isolated adipocytes were prepared by collagenase digestion (1 mg/ml) of adipose tissue.[14] Cells were resuspended in Krebs-Ringer bicarbonate buffer (KRB) containing 4% bovine serum albumin (BSA) and 200 nM adenosine[13] and incubated for 2 hours under an atmosphere of 95% O_2/5% CO_2 at 37^{o}C using the

following conditions: (1) in the presence of adenosine deaminase (ADA; 4 μg/ml) to assess 'disinhibited' basal lipolysis; (2) ADA + 1, 20, and 100 nM phenylisopropyl adenosine (PIA, an adenosine receptor agonist) to assess 'basal' lipolysis [These conditions may be more reflective of in vivo rates because the concentration of adenosine is approximately 130 μM (equivalent in potency to ~10 nM PIA).]; (3) ADA+ 20 nM PIA + 10, 100, and 1000 nM isoproterenol (ISO) to assess stimulated lipolysis; and (4) ADA + 7.9, 39, 78, 110 and 360 pM insulin to assess inhibition of lipolysis by insulin. After a 2-hour incubation at 37℃, media aliquot s were stored for measurement of glycerol[15] and non-esterified fatty acids (NEFA) (Wako Diagnostics, Richmond, VA). Data were expressed by cell number, cell size and mg of tissue.

Fat cell weight (FCW) was measured by averaging the diameters of at least 300 adipocytes from each biopsy sample using the photomicroscopic method of Lavau et al.[16] and surface area was calculated according to methods described by Leibel et al.[17] All measurements were made and analyzed blinded to *LIPE* genotype.

TG and diglyceride (DG) content in adipose tissue extracts was measured using thin layer chromatography (TLC).[18]

Protein quantitation:

~75 mg of adipose tissue was homogenized in adipose tissue buffer (45 mL Tris-EDTA buffer, 1 protease inhibitor tablet, 25 μL 0.2 M sodium orthovanadate, and 5 mL sodium fluoride), and protein was extracted using acetone. The pellet was re-suspended in Laemmli sample buffer (Biorad, Hercules, CA) and total protein was quantitated using the BCA Protein Assay Kit (Thermo Scientific, Rockford, IL). Equal amounts of protein (0.06 μg) were electrophoresed (10% SDS-PAGE), transferred to PVDF and immunoblotted with an antibody for the target gene. The amount of protein was quantified using a Fluorochem Q chemiluminescence imager (Protein Simple, Santa Clara, CA) and normalized to beta actin.[19] For quantitation of HSL protein, a human anti-HSL antibody provided by Cecilia Holm (Sweden) was used that binds the N-terminal portion of HSL and thus would be expected to recognize equally well the wild type and deletion forms of the protein.

RNA isolation and quantitation:

Adipose tissue was homogenized in 1 ml of Trizol (Invitrogen, Grand Island, NY) and total RNA was extracted according to the manufacturer's protocol. cDNA was synthesized using the Transcriptor First Strand cDNA Synthesis Kit (Roche, Basel, Switzerland). Steady state mRNA levels were determined by two-step quantitative real-time PCR (qRT-PCR) using the LightCycler 480 (Roche, Basel, Switzerland) and normalized to cyclophilin mRNA.[19] Primer sequences/assays are shown in Table S2.

Triglyceride lipase and cholesterol esterase activities:

Enzyme activity assays were performed as previously described.[20] Briefly, adipose tissue was prepared by homogenization in 0.25 M sucrose, 1 mM EDTA, and 1 mM DTT and was either combined with ^{14}C-cholesteryl oleate substrate or ^{3}H-triolein substrate and incubated at 37^{o}C for 1 hour. The reactions were stopped by adding 3.25mL methanol/chloroform/heptane (1:1:1) and 1.05mL (0.1 M potassium carbonate, 0.1 M boric acid) buffer at pH 10.5. Stopped reactions were centrifuged at 1500 rpm for 1 hour 20 minutes and ^{14}C and ^{3}H products partitioned into the upper phase were measured by liquid scintillation counting (Beckman Coulter, Brea, CA).

Retinyl ester quantification:

Normal phase HPLC analysis of retinyl esters in both serum and adipose tissue was as previously described.[21-23] Briefly, samples were separated using tandem 5 μm silica columns. Retinyl esters were separated in hexane:diethyl ether (99.6:0.4) at a flow rate of 0.8 ml/min. Retention times and spectral data were compared in retinol and retinyl esters (retinyl palmitate, oleate, linoleate, and stearate) of experimental compounds and those of authentic standards. The concentration of retinyl esters in the tissues were quantitated by comparing peak integrated areas for unknowns versus those of known concentrations of purified standards. Loss during extraction was adjusted for by the recovery of internal standard retinyl acetate added right after homogenization of the tissues.

Cloning of wild-type and mutant LIPE:

To generate human *LIPE* expression constructs, *LIPE* cDNA was amplified from the *LIPE* image clone #5296155 (NIH Mammalian Gene Collection; purchased from Invitrogen, Grand Island, NY) using primers containing the *HindIII* and *XbaI* restriction enzyme sites (forward primer: 5'-TCGCGGCCGCAAGCTTAACATGGACCTGCGCACAATGAC-3'; reverse primer: 5'-CATGCATCTAGAGCCAAACTAATTAAATACTTTTATTTAC-3') with high-fidelity Phusion polymerase (New England Biolabs, Ipswich, MA). The fragments were then cloned into a Gateway donor vector pEntra to make the wild-type vector pEntra-wt*LIPE*. The pEntra-mut*LIPE* construct was generated by site-directed mutagenesis of the pEntra-wt*LIPE* construct using Phusion polymerase with the mutation-containing primer pair (forward primer: 5'-GGCCGAGCGGGGAGACGGGGGCTGCGGGGGGCGACACTAAAAGCCTGTTGTTC-3'; reverse primer: 5'-AACAACAGGCTTTTAGTGTCGCCCCCCGCAGCCCCCGTCTCCCCGCT-3') followed by DpnI digestion and transformation. Sequencing of the full length cDNAs was used to verify the sequence of the wt*LIPE* construct and confirm proper mutagenesis in the generation of the mut*LIPE* construct.

In vitro expression of mutant LIPE:

For protein analysis, HEK293 cells were cultured in DMEM (Invitrogen, Grand Island, NY) supplemented with 10% iron-supplemented calf serum, 100 U/ml penicillin G sodium, and 100 mg/ml streptomycin sulfate (Invitrogen, Grand Island, NY) and transfected with wt*LIPE* or mut*LIPE* expression vectors. Cells were cultured in the presence or absence of proteosomal inhibitor MG132 (10 uM) or MG132 (10 uM) and leupeptin (10ug/mlfor 8-24 hours. Cells were washed with PBS and lysed cold RIPA buffer. Equal amounts of protein (0.06 µg) were electrophoresed (10% SDS-PAGE), transferred to nitrocellulose and immunoblotted with an HSL (Cell Signaling, Danvers, MA) antibody. The blots were quantified using a Fluorochem Q chemiluminescence imager (Protein Simple, Santa Clara, CA) and normalized to GAPDH (Proteintech, Chicago, IL).

Histology and imaging:

Paraffin-embedded adipose tissue sections were deparaffinized, rehydrated, and immersed in methanol containing 0.3% H_2O_2 for 30 minutes to exhaust endogenous peroxidase activity. The sections were incubated in 10% normal horse serum for 20 minutes at room temperature followed by incubation with anti-HAM56 (1:50) for 1 hour. Biotinylated secondary antibody was applied for 30 minutes. The slides were washed in PBS, incubated with ABC reagent for 30 minutes (Vector Laboratories, Inc., Burlingame, CA.), and developed with 3, 3-diaminobenzidine (DAB) for 4 minutes. The sections were then counterstained with hematoxylin. After mounting the coverslip, the sections were visualized using light microscopy.[24]

Acute cytokine release:

Acute cytokine release was measured from 100 mg of adipose tissue in 1.5 ml media (sterile M199 1% BSA) after gassing with 95% O_2/5% CO_2. Samples were incubated at 37^{o}C for 3 hours. The reaction was terminated on ice. The media was removed and frozen at -80^{o}C. TNFα and IL-6 levels were measured using ELISA (R&D Systems, Inc., Minneapolis, MN).

Statistical analysis:

Association analyses of quantitative traits were performed using the measured genotype approach that models variation in the trait of interest as a function of measured environmental covariates, measured genotype and a polygenic component to account for phenotypic correlation due to relatedness. A t-test was used to assess significance of the measured genotype beta coefficient. We included sex and age as covariates and coded the SNPs using an additive model. The polygenic component was modeled using the relationship matrix derived from the complete 14-generation pedigree structure to properly control for the relatedness of all subjects in the study. These analyses were carried out using the mixed model software MMAP developed in our group.[25]

Traits examined include serum lipids (i.e. total cholesterol, HDL-cholesterol, LDL-cholesterol, and TG), insulin and glucose after fasting and during an oral glucose tolerance test (when available) and hepatic fat content. Fasting insulin, glucose measures and HOMA-IR (skewed traits) were log transformed before analysis and untransformed means were reported for ease of interpretation. Differences in serum measurements and adipose tissue deposition variables among the siblings in the proband pedigree were compared using the Wilcoxon/Kruskal-Wallis ranked sum test. Correlation between body fat and serum leptin levels was assessed using Spearman correlation.

Differences in mRNA and protein levels, enzyme activity, adipocyte size, and lipolysis between mutant and wild type adipose tissue were all compared using a single factor ANOVA. For adipocyte size (Fig. S6) and insulin sensitivity (Fig. S8A), each point was compared separately using the same method. All p-values are two-sided and a p-value of 0.05 or below was considered statistically significant.

Findings from Physical Examination of Proband Family:

The proband and 7 of her siblings were examined by the same physician (ARS). Overall, the physical exams were unremarkable for major abnormalities. General appearance, head, ears, eyes nose and throat were normal. The skin exams revealed no acanthosis nigricans or hirsuitism. Lungs were clear to percussion and auscultation. All had normal heart rate and regular rhythm, with normal heart sounds and no evidence of cardiomegaly or heart failure. Peripheral pulses were normal and without bruits. Abdominal exams were normal without evidence of hepatomegaly, except for Subject 3 (see below). Musculoskeletal exams were normal and neurological exams were non-focal. Other subject-specific findings include (also see Figure 1B):

Pedigree Subject 1 (Proband; DD homozygote; female): BP 128/75 mmHg, P 72 bpm, BMI 27 kg/m^2. Mild increase in fat deposition under the chin (double chin). Neck and upper extremity subcutaneous fat normal; lower extremity subcutaneous fat appeared decreased.

Pedigree Subject 3 (DD homozygote; female): BP 118/58 mmHg, P 80 bpm, BMI 27 kg/m^2. Vitiligo on hands, arms and legs. Liver was palpable 2 cm below the right costal margin. There was little or no fat on the lower extremities with normal trunkal fat amount and distribution.

Pedigree Subject 4 (ID heterozygote; female): BP 120/65 mmHg, P 68 bpm, BMI 31 kg/m^2. Mild/moderate decrease in hearing on the right (history of recurrent right ear otitis media). Dry scaly lesion over left knee. Mild to moderate increase in fat deposition under the chin (double chin; even noted by others when she was younger). Relative decrease in subcutaneous fat in lower extremities.

Pedigree Subject 5 (ID heterozygote; female): BP 120/76 mmHg, P 78 bpm, BMI 23 kg/m^2. Extremities with little or no adipose tissue. Small amount of fat in abdominal and hip regions.

Pedigree Subject 6 (II homozygote; female): BP 131/78 mmHg, P 80 bpm, BMI 23 kg/m^2. Presence of arcus senilis. Mild increase in fat deposition under the chin (double chin). Extremities with little or no adipose tissue. Small amount of fat in abdominal and hip regions.

Pedigree Subject 8 (ID heterozygote; male): BP 112/78 mmHg, P 64 bpm, BMI 22 kg/m^2. Extremities with little or no adipose tissue. Trunkal fat distribution appears normal.

Pedigree Subject 9 (II homozygote; male): BP 106/66 mmHg, P 64 bpm, BMI 24 kg/m^2. No obvious abnormalities in body fat distribution.

Pedigree Subject 10 (II homozygote: male): BP 136/86 mmHg, P 64 bpm, BMI 29 kg/m^2. Presence of arcus senilis. Mild to moderate decrease in hearing on the right. Normal appearing fat distribution.

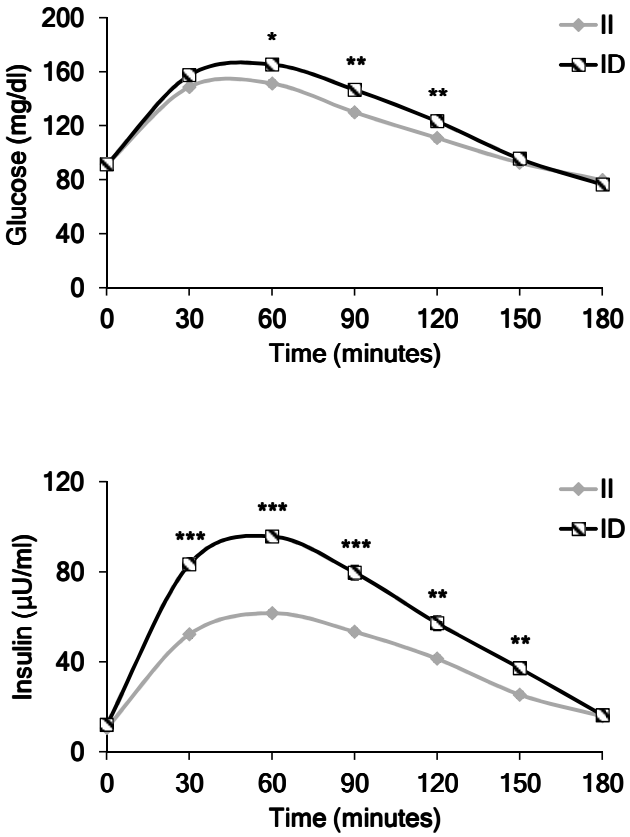

Figure S1: Association of the *LIPE* mutation with impaired glucose and insulin metabolism. Serum glucose (upper panel) and insulin levels (lower panel) in non-diabetic subjects (N: II=716 and ID=35) measured during a 3-hour oral glucose tolerance test. Total glucose (gAUC) and insulin area under the curve (iAUC) were higher in ID compared to II subjects ($p = 0.02$ and $p = 2.5 \times 10^{-5}$, respectively), suggesting that HSL haploinsufficiency results in insulin resistance. Type 2 diabetes was defined by fasting plasma glucose level ≥ 126 mg/dl, random or 2-hour OGTT glucose ≥ 200 mg/dl, the use of insulin or prescription oral glucose-lowering agents, or a previous diagnosis of diabetes documented by a physician. 51.6% of subjects were females. Mean age and BMI were 44 years and 26.9 kg/m^2, respectively. Analyses were adjusted for age, sex, and family structure.

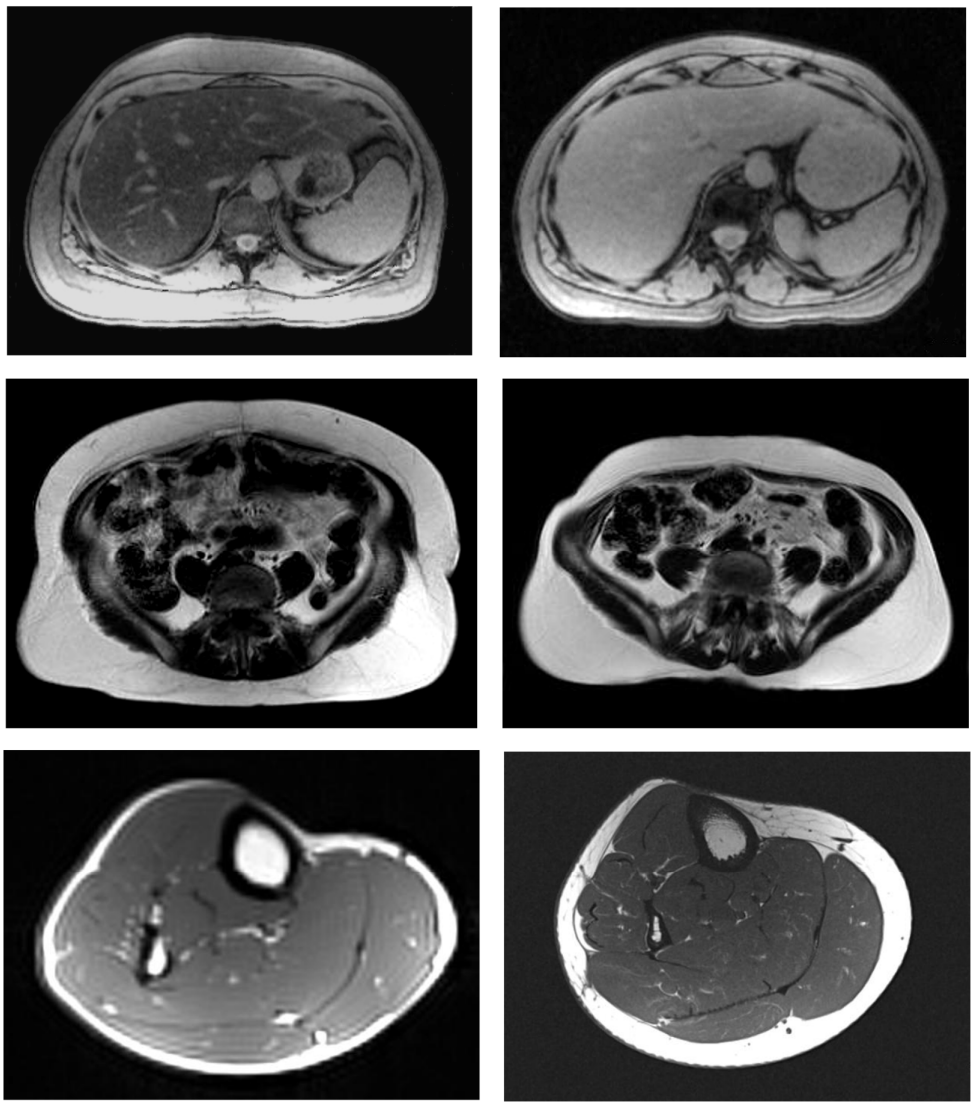

Figure S2: Evidence by magnetic resonance imaging (MRI) for redistribution of body fat in a DD compared to an II subject. Representative images from MRI of liver, abdomen and calf for pedigree sibling #3 (DD for the HSL mutation; left panel) and pedigree sibling #6 (II for the HSL mutation; right panel). Images are not necessarily to scale. The upper panel shows images of the liver obtained using identical scan parameters. The pulse sequence takes advantage of the different precessional frequencies of fat and soft tissue protons; the higher the percentage of fat, the darker the appearance of the tissue. The liver on the left, in which hepatic fat content is quite high (25.3%), has a darker appearance than the liver on the right, where the hepatic fat content is normal (2.8%). The middle panel shows images of the abdomen obtained at the L4-5 disk space from DD (left) and II (right) subjects. The images have been digitally manipulated such that any bright signal in the image is fat. Fat can be seen both subcutaneously and within the viscera. The DD individual has a higher amount of visceral fat compared to the II (89.0 cm^2 vs. 77.3 cm^2, respectively). The lower panel shows images of the right calf obtained where the soleus muscle is most thick. The bright (white) subcutaneous tissue is fat. Subcutaneous fat in calf of DD subject (7.7 cm^2) (left) is substantially reduced compared to that of the II subject (21.5 cm^2) (right), resulting in a significant increase in the abdominal:calf subcutaneous fat ratio in the DD compared to II subject (41.4 vs. 9.9, respectively).

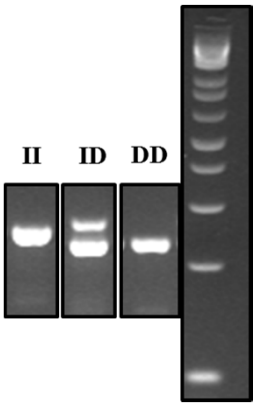

Figure S3: Evidence at the mRNA level of the frameshift mutation. Representative amplification of cDNA from subcutaneous abdominal adipose tissue of individuals with II, ID, and DD genotypes shows amplicons that differ in size by approximately 19 base pairs. II and DD bands are approximately 253 and 234 base pairs, respectively. 100 bp DNA Ladder (Life Technologies, Grand Island, NY) was used as a size reference.

A.

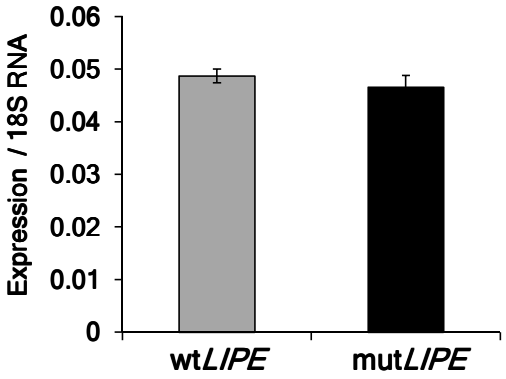

B.

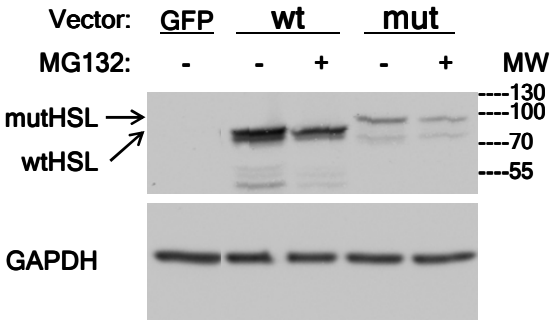

Figure S4: Expression of mutant *LIPE* in HEK293 cells replicates *in vivo* observations. (A) No difference in mRNA expression of wild-type (wt*LIPE*) and mutated (mut*LIPE*) *LIPE* cDNA constructs. 24 hours after transfection, HEK293 cells were collected for RNA isolation and qRT-PCR. Two independent experiments were conducted in duplicate for each the wt*LIPE* and mut*LIPE* (n = 4). **(B)** Mutated HSL protein expression was markedly reduced compared to wt protein (representative blot of two independent experiments). HEK293 cells were transiently transfected with plasmid vectors for the expression of GFP (control), wt*LIPE*, or mut*LIPE* constructs for 48 hours. Cells were treated or not with MG132, a proteosomal inhibitor (10µM), for the last 8 hours. Inhibition of proteosomal degradation using MG132 did not significantly alter wt or mutant protein levels in time courses up to 24 hours (data not shown). Similar results were also shown using the lysosomal inhibitor leupeptin (10 mg/ml) (data not shown). In subcutaneous abdominal adipocytes from ID and DD subjects no mutant protein was detected (Fig. 2B); however, traces of the mutant protein were observed in the in vitro system as shown above, but were likely due to forced overexpression and/or differences in cell type-specific post-transcriptional regulation (e.g. adipocytes vs. HEK293 cells). These findings suggest decreased translation and/or instability of the mutant HSL protein.

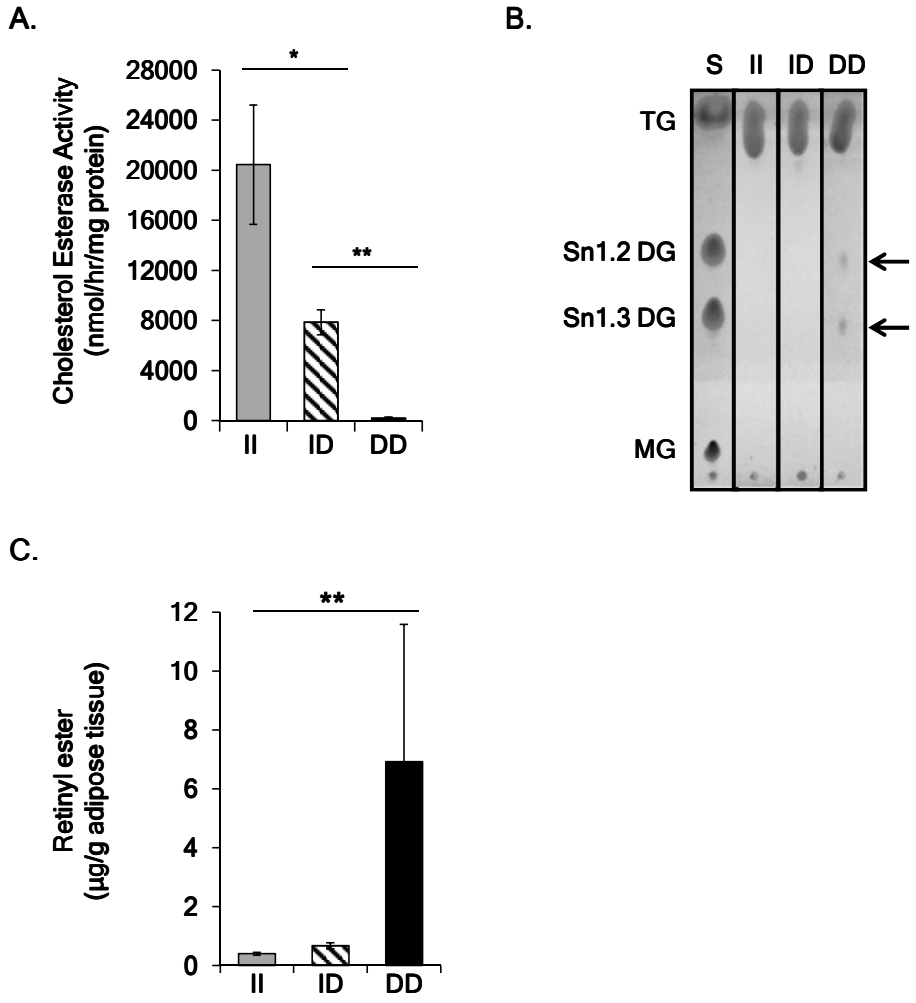

Figure S5: Reduced hydrolytic activities in HSL null subcutaneous abdominal adipose tissue. **(A)** *In vitro* hydrolytic activity against cholesterol ester (CE) was measured in adipose tissue homogenates; a dose-dependent reduction in CE hydrolase activity in D allele carriers was observed, corroborating a correlation between protein level and enzymatic activity. **(B)** Lipids from adipose tissue of subjects with all three genotypes were extracted. Triacylglycerol equivalent to 300 µg were analyzed by thin-layer chromatography. A mixture of triglyceride (TG), *sn*-1.2/1.3 diglyceride (DG), and monoglyceride (MG) was used as a standard (S). Lipids were visualized using iodine. Arrows denote accumulation of DG in the DD subject. (N: II = 2, ID = 2 and DD = 2) **(C)** Reverse phase HPLC separation and quantification of total retinyl ester (RE) showed accumulation of RE in adipose tissue from DD subjects. (N: II = 7, ID = 10 and DD = 2; *$p < 0.05$, **$p < 0.01$, ***$p < 0.001$) Data are the mean ± SEM.

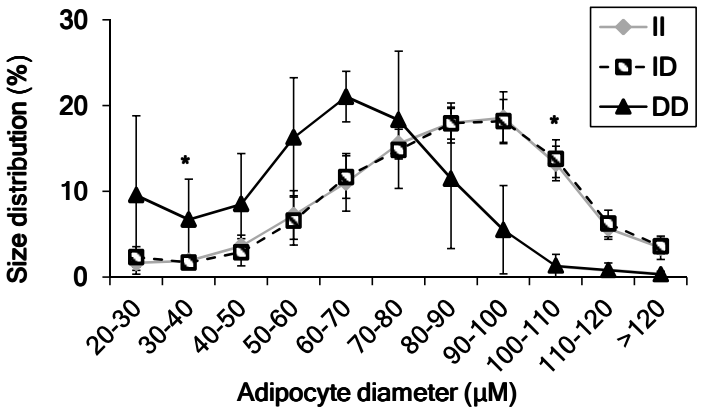

Figure S6: Reduced adipocyte size in HSL null subcutaneous abdominal adipose tissue. Diameters of 300 cells from adipocyte suspension prepared from biopsy samples from each II, ID and DD subject were measured using a microscope with an ocular micrometer. Adipocyte size distribution represented as percentage of cell size per total number of cells counted. Mean diameter was significantly smaller in DD (60.8 ± 14.8 µm) compared to II (85.6 ± 2.02 µm) subjects (DD vs. II: p=0.02).

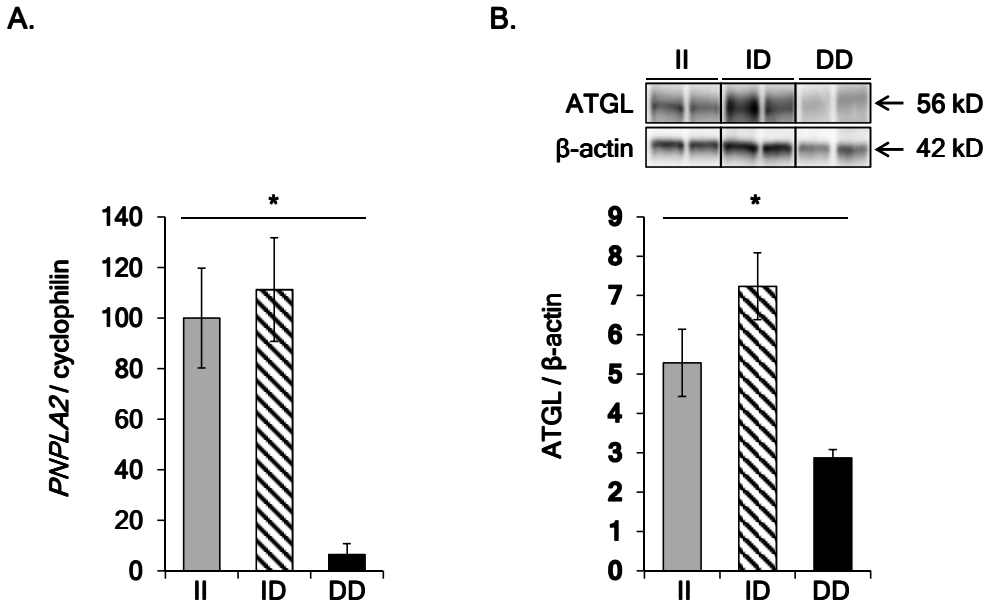

Figure S7: Reduced mRNA and protein levels of adipose triglyceride lipase (ATGL) in HSL null subcutaneous abdominal adipose tissue. (A) *PNPLA2* mRNA was measured using quantitative real-time PCR (qRT-PCR) and normalized to cyclophilin. (N: II = 7, ID = 10 and DD = 2) **(B)** ATGL protein levels were measured from whole tissue extracts using Western blot analysis and normalized to β-actin. Reduced mRNA and protein levels of ATGL exacerbated further the lipolytic defect observed in HSL null adipocytes, indicating no compensatory action of ATGL in response to absence of HSL. (N: II = 5, ID = 5 and DD = 2; *$p < 0.05$, **$p < 0.01$, ***$p < 0.001$) Data are the mean ± SEM.

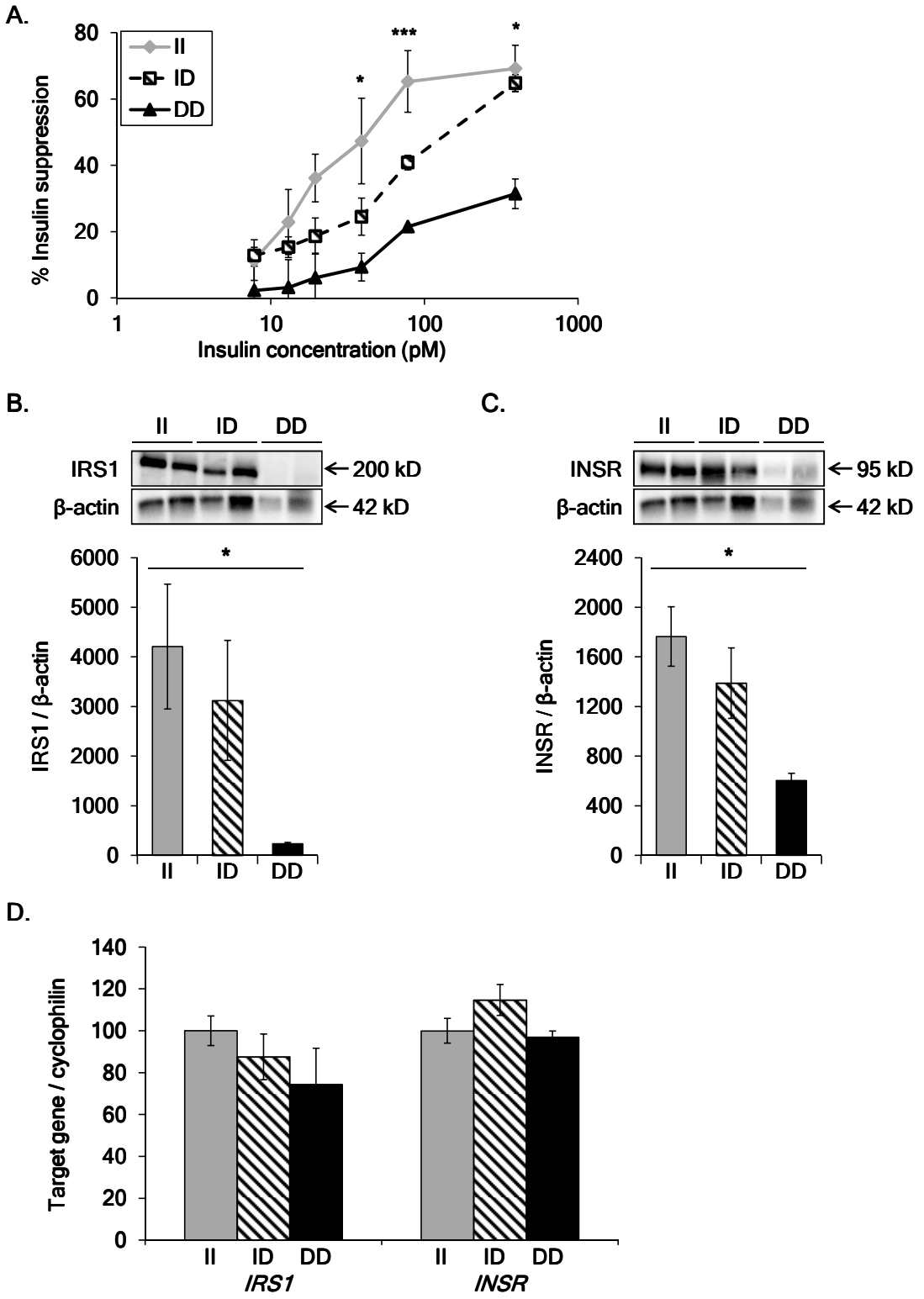

Figure S8: Evidence for insulin resistance in HSL null subcutaneous abdominal adipose tissue. **(A)** Sensitivity to the antilipolytic effect of insulin was decreased in DD and ID compared to II adipocytes, whereas maximal response to insulin was reduced ~50 in DD compared to II adipocytes, indicating insulin resistance. Insulin-suppressed lipolysis, expressed as percent suppression, was measured by incubating isolated adipocytes with adenosine deaminase (ADA) or ADA + insulin concentrations of 7.9, 39, 78, 110 and 390 pM. Reduced protein levels of **(B)** insulin receptor substrate 1 (IRS1) and **(C)** insulin receptor (INSR) in HSL null adipose tissue may be contributing to insulin resistance. Protein levels were measured from whole tissue extracts by Western blot analysis using antibodies provided by Michael Quon and Xiao Jian Sun and normalized to β-actin. (N: II = 5, ID = 5 and DD = 2). **(D)** mRNA levels of *IRS1* and *INSR* were measured using qRT-PCR and normalized to cyclophilin. (N: II = 7, ID = 10 and DD = 2; *p < 0.05, **p < 0.01, ***p < 0.001). Data are the mean ± SEM.

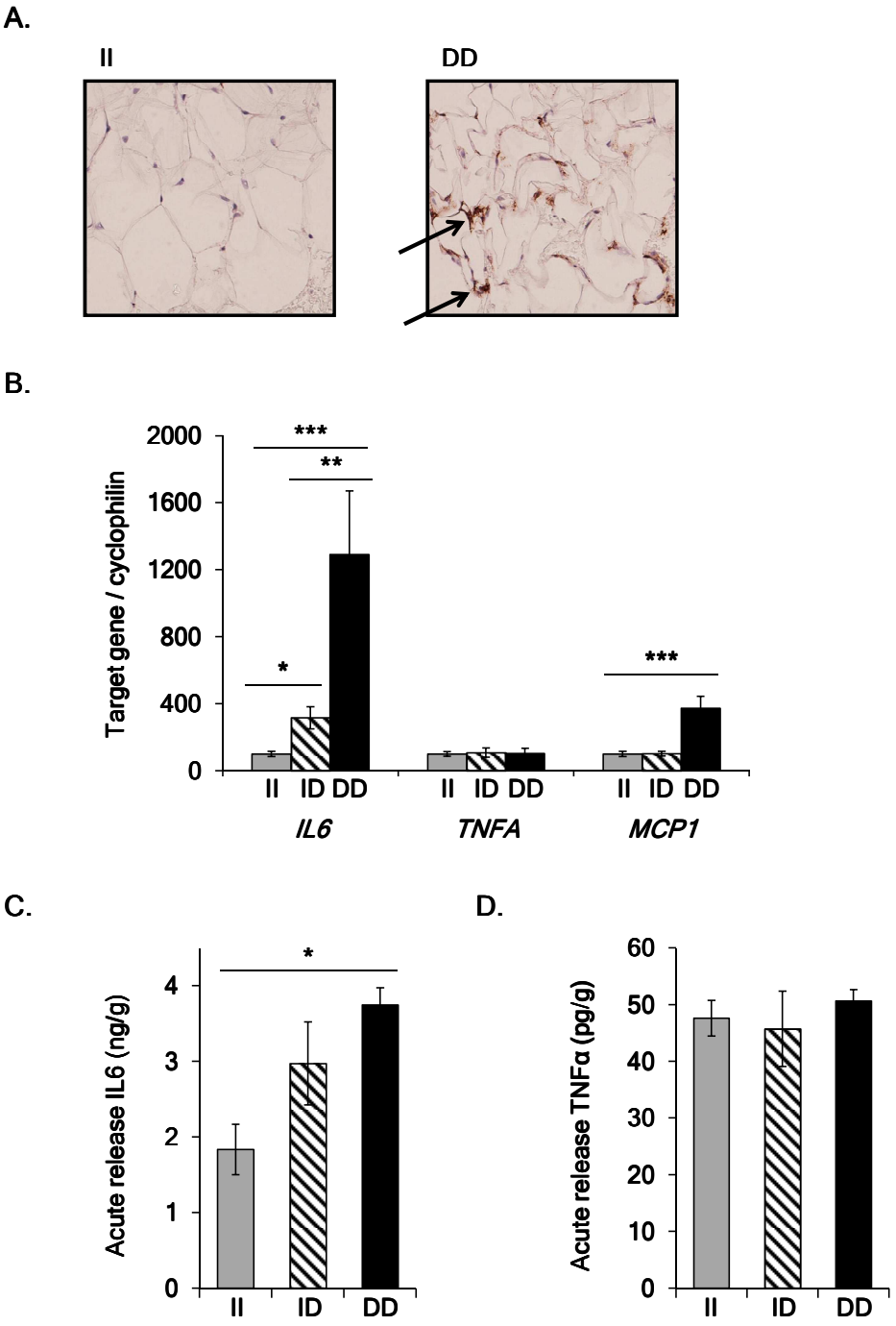

Figure S9: Evidence for inflammation in HSL null subcutaneous abdominal adipose tissue. (A) Absence of HSL resulted in histological abnormalities with an increase in macrophage infiltration, a hallmark of inflammation, in DD adipocytes. HAM56 macrophage staining of paraffin embedded formalin fixed adipose tissue in an II and a DD subject. Black arrows denote examples of macrophage infiltration in the DD adipose tissue. **(B)** Increased mRNA expression of pro-inflammatory cytokines interleukin-6 (*IL6*) and macrophage chemokine protein-1 (*MCP1*) were also observed in HSL null adipose tissue. mRNA levels of *IL6*, tumor necrosis factor-alpha (*TNFA*) and *MCP1* were measured using qRT-PCR and normalized to cyclophilin. The acute release from adipose tissue into media of **(C)** IL6 (higher in D allele carriers) and **(D)** TNFα was measured using an ELISA kit. (N: II = 7, ID = 10 and DD = 2; *p < 0.05, **p < 0.01, ***p < 0.001) Data are the mean ± SEM.

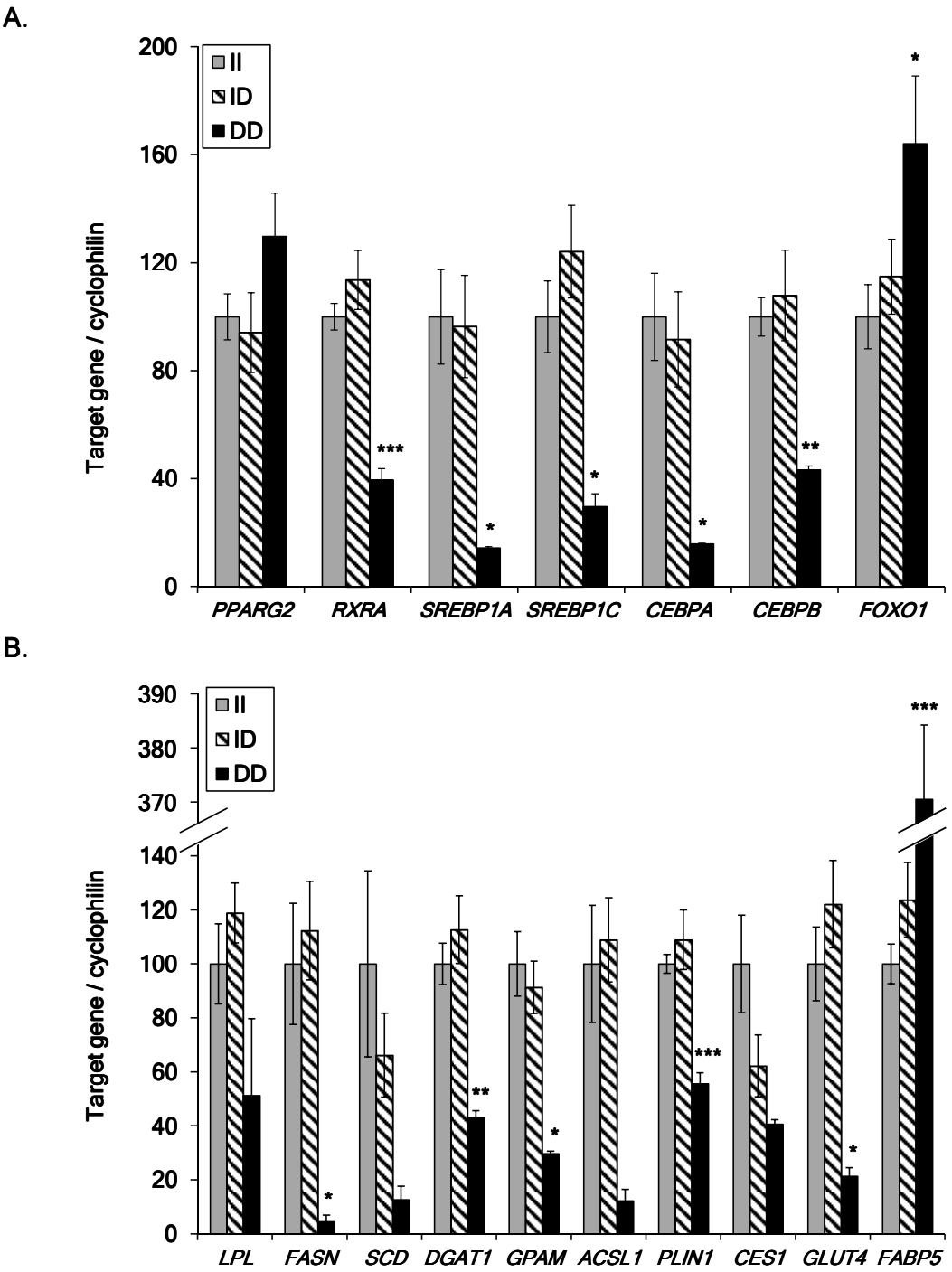

Figure S10: Altered transcriptional regulation of genes involved in adipogenesis, maintenance of adipocyte function, and lipid and glucose metabolism in HSL null white adipose tissue (WAT). (A) No change in mRNA levels of *PPARG2*, but marked reduction in mRNA levels of *RXRA* (-61%), the obligate heterodimer partner required for activation of the PPARγ pathway, and other critical transcription regulators of terminal differentiation [sterol regulatory element-binding factor-1a (*SREBP1A*): -86%; *SREBP1C*: -70%; CCAAT/enhancer-binding protein α (*CEBPA*): -84%; *CEBPB*: -57%] in HSL null WAT. **(B)** Downregulation of mRNA levels of downstream target genes involved in multiple lipid and glucose metabolic pathways in DD compared to II WAT: FFA uptake [e.g. lipoprotein lipase (*LPL*): -50%], FFA synthesis [e.g. fatty acid synthase (*FASN*): -95%; stearoyl-CoA desaturase (*SCD*): -87%], TG synthesis [e.g. acyl-CoA:diacylglycerol acyltransferase-1 (*DGAT1*): -57%; glycerol-3-phosphate acyltransferase (*GPAM*): -73%; acyl-CoA synthetase-1 (*ACSL1*): -88%], lipolysis [e.g. perilipin 1 (*PLIN1*): -45%; carboxylesterase (*CES1*): -60%], and glucose transport [e.g. glucose transporter 4 (*GLUT4*): -79%] in HSL null WAT. mRNA levels were measured using qRT-PCR and normalized to cyclophilin. (N: II = 7, ID = 10 and DD = 2; *$p < 0.05$, **$p < 0.01$, ***$p < 0.001$) Data are the mean ± SEM.

Table S1: Body composition by DXA in subjects matched for total body percent fat (± 2.5%) and sex (female) to the DD females.

	II	ID	DD Subject #			
	N = 42	N = 7	1	2	3	
DXA Region	**Mean (SE)**	**Mean (SE)**	**Value**	**Value**	**Value**	**p-value***
Age (Years)	43 (5)	43 (11)	40	46	56	
Whole Body Percent Fat	32.1% (1.2%)	32.4% (1.9%)	31.3	33.2	33.6	0.61
Android Percent Fat	26.0% (4.0%)	28.9% (4.3%)	32.2	36.8	34.5	0.002
Gynoid Percent Fat	39.1% (2.5%)	40.4% (3.1%)	36.4	34.5	33.9	0.001
Leg Percent Fat	40.0 % (2.7%)	38.9% (2.0%)	33.4	30.8	26.1	2.1×10^{-6}
Upper Leg Percent Fat	38.6% (2.3%)	39.4% (2.3%)	34.2	32.7	30.2	1.5×10^{-5}
Lower Leg Percent Fat	38.3% (4.3%)	36.0% (3.8%)	29.9	23.9	16.1	2.7×10^{-5}
Arm Percent Fat	32.7% (3.7%)	33.5% (3.9%)	41.3	38.2	38.7	0.04

* p-value = recessive model (II/ID vs. DD) adjusted for age and family structure; no statistically significant difference between the II and ID genotype group means were observed ($p > 0.16$)

Table S2: Primer pairs/assays for qRT-PCR for each gene.

Gene	Forward*	Reverse
ACSL1	cgacttcaccaactggttctg	atgcaggttgtgcgatca
ATGL	cgctctgtccttcaccatct	cgcgcatcaccaggtact
CEBPA	agttcctggccgacctgt	cccgggtagtcaaagtcg
CEBPB	Hs00270923_s1	
CES1	gtggctccgtgcctttatc	acggtgtccaccacaggt
Cyclophilin	Hs99999904_m1	
DGAT1	Hs00201385_m1	
FABP5	gcagacccctctctgcac	tcgcaaagctattcccactc
FASN	caggcacacacgatggac	cggagtgaatctgggttgat
FOXO1	aagggtgacagcaacagctc	ttctgcacacgaatgaacttg
GLUT4	ctgtgccatcctgatgactg	cgtagctcatggctggaact
GPAM	ggaaagtttatccagtatggcatt	tgatatcttcctggtcatcgtg
HSL	cgctggaggagtgcttctt	ttcgttcccctgttgagc
IL-6	Hs00174131_m1	
INSR	Hs00961554_m1	
IRS1	Hs00178563_m1	
LPL	ggcgtgaaaacagtgtcaga	gctagaagtgggcagctttc
MCP-1	Hs00234140_m1	
PLIN1	ggacacagtggtgcattacg	gtcccggaattcgctctc
PPARD	cggtgttcatgcatgtgag	agctgcgctcacacttctc
PPARG2	Hs01115510_m1	
RXRA	Hs01067640_m1	
SCD	cctagaagctgagaaactggtga	acatcatcagcaagccaggt
SREBP1A	cgctcctccatcaatgaca	tgcgcaagacagcagattta
SREBP1C	Hs01088691_m1	
TNFA	cagcctcttctccttcctgat	gccagagggctgattagaga

* Hs numbers refer to primer/probe assays by Life Technologies (Grand Island, NY)

SUPPLEMENTAL REFERENCES

1. Lee WJ, Pollin TI, O'Connell JR, Agarwala R, Schaffer AA. PedHunter 2.0 and its usage to characterize the founder structure of the Old Order Amish of Lancaster County. BMC Med Genet 2010;11:68.
2. Hsueh WC, Mitchell BD, Aburomia R, et al. Diabetes in the Old Order Amish: characterization and heritability analysis of the Amish Family Diabetes Study. Diabetes Care 2000;23:595-601.
3. Post W, Bielak LF, Ryan KA, et al. Determinants of coronary artery and aortic calcification in the Old Order Amish. Circulation 2007;115:717-24.
4. Mitchell BD, Hsueh WC, King TM, et al. Heritability of life span in the Old Order Amish. Am J Med Genet 2001;102:346-52.
5. Mitchell BD, McArdle PF, Shen H, et al. The genetic response to short-term interventions affecting cardiovascular function: rationale and design of the Heredity and Phenotype Intervention (HAPI) Heart Study. Am Heart J 2008;155:823-8.
6. Shuldiner AR, O'Connell JR, Bliden KP, et al. Association of cytochrome P450 2C19 genotype with the antiplatelet effect and clinical efficacy of clopidogrel therapy. JAMA 2009;302:849-57.
7. Friedewald WT, Levy RI, Fredrickson DS. Estimation of the concentration of low-density lipoprotein cholesterol in plasma, without use of the preparative ultracentrifuge. Clin Chem 1972;18:499-502.
8. Genuth S, Alberti KG, Bennett P, et al. Follow-up report on the diagnosis of diabetes mellitus. Diabetes Care 2003;26:3160-7.
9. Grundy SM, Cleeman JI, Daniels SR, et al. Diagnosis and management of the metabolic syndrome: an American Heart Association/National Heart, Lung, and Blood Institute Scientific Statement. Circulation 2005;112:2735-52.
10. Third Report of the National Cholesterol Education Program (NCEP) Expert Panel on Detection, Evaluation, and Treatment of High Blood Cholesterol in Adults (Adult Treatment Panel III) final report. Circulation 2002;106:3143-421.
11. Speliotes EK, Yerges-Armstrong LM, Wu J, et al. Genome-wide association analysis identifies variants associated with nonalcoholic fatty liver disease that have distinct effects on metabolic traits. PLoS Genet 2011;7:e1001324.
12. Yokoo T, Bydder M, Hamilton G, et al. Nonalcoholic fatty liver disease: diagnostic and fat-grading accuracy of low-flip-angle multiecho gradient-recalled-echo MR imaging at 1.5 T. Radiology 2009;251:67-76.
13. Johnson JA, Fried SK, Pi-Sunyer FX, Albu JB. Impaired insulin action in subcutaneous adipocytes from women with visceral obesity. Am J Physiol Endocrinol Metab 2001;280:E40-9.
14. Honnor RC, Dhillon GS, Londos C. cAMP-dependent protein kinase and lipolysis in rat adipocytes. I. Cell preparation, manipulation, and predictability in behavior. J Biol Chem 1985;260:15122-9.
15. Laurell S, Tibbling G. An enzymatic fluorometric micromethod for the determination of glycerol. Clin Chim Acta 1966;13:317-22.
16. Lavau M, Susini C, Knittle J, Blanchet-Hirst S, Greenwood MR. A reliable photomicrographic method to determining fat cell size and number: application to dietary obesity. Proc Soc Exp Biol Med 1977;156:251-6.
17. Leibel RL, Hirsch J. Site- and sex-related differences in adrenoreceptor status of human adipose tissue. J Clin Endocrinol Metab 1987;64:1205-10.
18. Folch J, Lees M, Sloane Stanley GH. A simple method for the isolation and purification of total lipides from animal tissues. J Biol Chem 1957;226:497-509.
19. de Souza Batista CM, Yang RZ, Lee MJ, et al. Omentin plasma levels and gene expression are decreased in obesity. Diabetes 2007;56:1655-61.
20. Holm C, Osterlund T. Hormone-sensitive lipase and neutral cholesteryl ester lipase. Methods Mol Biol 1999;109:109-21.
21. Wei S, Episkopou V, Piantedosi R, et al. Studies on the metabolism of retinol and retinol-binding protein in transthyretin-deficient mice produced by homologous recombination. J Biol Chem 1995;270:866-70.
22. Blaner WS, Das SR, Gouras P, Flood MT. Hydrolysis of 11-cis- and all-trans-retinyl palmitate by homogenates of human retinal epithelial cells. J Biol Chem 1987;262:53-8.
23. Quadro L, Hamberger L, Gottesman ME, Colantuoni V, Ramakrishnan R, Blaner WS. Transplacental delivery of retinoid: the role of retinol-binding protein and lipoprotein retinyl ester. Am J Physiol Endocrinol Metab 2004;286:E844-51.
24. Ranganathan S, Noyes NC, Migliorini M, et al. LRAD3, a novel low-density lipoprotein receptor family member that modulates amyloid precursor protein trafficking. J Neurosci 2011;31:10836-46.

25. O'Connell JR. Optimizing measured genotype genome-wide association analysis for quantitative traits in pedigrees. In. Philadelphia, PA; 2008.